

Combinatorial Design of Novel Multiprincipal Element Alloys Using Experimental Techniques

Jenő Gubicza

Multiprincipal element alloys (MPEAs) including high-entropy alloys are in the focus of materials science since many MPEA compositions exhibit outstanding mechanical and physical properties. These alloys contain 3–6 constituents with similar fractions; therefore, MPEAs correspond to the unexplored middle part of the phase diagrams. The phase composition and the performance of MPEAs are strongly influenced by their chemistry. Thus, it is very important to reveal the correlation between the composition, the structure, and the properties of MPEAs. On the other hand, this task is challenging due to the vast composition space of these alloys. The processing and characterization of combinatorial specimens can yield a fast mapping of compositional libraries of MPEAs. Herein, the experimental techniques developed for manufacturing and investigation of these alloys are overviewed and the results are critically discussed. Finally, further development directions in the field of combinatorial MPEAs are recommended in order to improve the study of the different alloy compositions.

universal gas constant) which can stabilize the multicomponent single-phase structure. The idea of HEAs is based on bulk metallic glasses (BMGs) also consisting of 4–5 major elements and exhibiting exceptionally high specific strength.^[4] Many HEAs show similarly high specific strength as BMGs but in addition HEAs also exhibit a considerable ductility since they are crystalline substances while BMGs have very limited plasticity during deformation due to their amorphous structures.^[4] The high hardness and strength of MPEAs can be attributed mainly to the strong resistance of the disordered multicomponent crystal lattice to dislocation motion.^[5] Refractory MPEA compositions (e.g., V–Nb–Mo–Ta–W) may have even a higher yield strength than Ni-based superalloys at temperatures higher than 1000 °C.^[6,7]

1. Introduction

Multiprincipal element alloys (MPEAs) contain three or more elements with similar compositions; therefore, this alloy concept differs significantly from the conventional one where there is one principal element (solvent) and the other constituents (solutes) are added with minor fractions.^[1,2] MPEAs are also called as compositionally complex alloys since they represent the unknown middle part of the multicomponent phase diagrams.^[1] Thus, MPEAs may have an exceptional combination of properties, opening the door to their innovative applications. High-entropy alloys (HEAs) is a subclass of MPEAs: these alloys have a minimum of five principal elements with atomic concentrations ranging from 5 to 35%.^[3] The fulfillment of this criterion yields a high configuration entropy (higher than $1.61 R$, where R is the

MPEAs exhibit exceptional properties among metallic materials such as the very high strength and wear resistance as well as the elevated hydrogenation rate and hydrogen storage capacity.^[8–10] The properties of MPEAs are significantly influenced by their chemical compositions.^[11] Many distinct MPEAs can be made due to the wide range of selectable chemical components. Furthermore, the concentrations of a particular group of elements may be changed, resulting in significantly diverse structures and a wide range of MPEA properties.^[12,13] If the component elements are selected, the study of the effect of chemical composition on the structure and properties of MPEAs would require to produce a significant number of samples. Instead, mapping of the structure and properties in a compositional library is easier when a combinatorial specimen is utilized.^[14] Using fast characterization techniques such as synchrotron X-ray diffraction (XRD) and instrumented indentation on combinatorial samples, the correlation between the composition and the features of MPEAs can be successfully revealed.^[15] In this study, former experimental results obtained on the processing and characterization of combinatorial MPEAs are critically overviewed and the envisioned future research directions in this field are described. It should be noted that in addition to the experimental techniques, modern theoretical methods (e.g., machine learning [ML], molecular dynamics [MD], density functional theory (DFT) calculations and CALPHAD modeling) have also been applied to predict the correlation between the chemical composition, phase composition, and properties of MPEAs.^[16–21] In addition, they are useful in narrowing the compositional space needed to study


J. Gubicza

Department of Materials Physics

ELTE Eötvös Loránd University

P.O.B. 32, H-1518 Budapest, Hungary

E-mail: jeno.gubicza@ttk.elte.hu

 The ORCID identification number(s) for the author(s) of this article can be found under <https://doi.org/10.1002/adem.202301673>.

© 2023 The Authors. Advanced Engineering Materials published by Wiley-VCH GmbH. This is an open access article under the terms of the Creative Commons Attribution-NonCommercial License, which permits use, distribution and reproduction in any medium, provided the original work is properly cited and is not used for commercial purposes.

DOI: 10.1002/adem.202301673

experimentally if an MPEA is searched for a desired property combination. However, in this study, I focus on the experimental design of combinatorial MPEAs and less attention is paid to the complementary theoretical methods.

2. Processing of Combinatorial MPEAs

Different experimental techniques have been proposed in the literature for producing combinatorial MPEA samples. These are the following methods: 1) heat treatment of diffusion couples, 2) processing of combinatorial films by sputtering of different elemental sources, and 3) additive manufacturing (AM) of powders with different compositions.^[22–26] During the first method, a homogeneous MPEA sample is placed in physical contact with a specimen made of a pure foreign element (e.g., the diffusion couple may be a CoNiCrMo MPEA and a pure Fe) and then annealed at an elevated temperature and under an inert Ar gas atmosphere in order to initiate interdiffusion between them.^[25] As a result of this procedure, a compositional library develops at the interface of the two samples. An advantage of this technique is that the processing conditions are more suitable to achieve an equilibrium phase composition at the different element concentrations compared to the other two methods (sputtering and AM). On the other hand, the compositional gradient is limited to a thin region with a thickness of about 200 μm in the close vicinity of the interface of the diffusion couples. Therefore, 1 at% change in concentration of the alloying element in this gradient region corresponds to a distance of $\approx 2\text{--}3\ \mu\text{m}$ only. Thus, the characterization of the change of the phase composition versus the element concentrations is not feasible by laboratory XRD due to the large beam size (about 1 mm), although this would be the fastest and easiest way for structural mapping of a combinatorial sample.

Contrary to diffusion couples, for combinatorial films processed by physical vapor deposition (PVD) techniques, the phase mapping can be easily performed by XRD due to larger sample size and the lower concentration gradient.^[15,22] For instance, in the case of a Co–Cr–Fe–Ni combinatorial MPEA layer processed by multiple-beam sputtering (MBS), the chemical composition changed with 1 at% at a distance of 2–3 mm which is one order of magnitude larger than that for diffusion couples.^[15] Therefore, a phase map can be obtained quickly by synchrotron XRD. An important advantage of combinatorial films produced by MBS is that it is obtained using pure elemental sputtering sources placed around the substrate disk; therefore, a very extended compositional library develops compared to diffusional couples where usually only the concentration of the foreign element changes in a wide range while the fractions of the elements in the MPEA member of the diffusion couple only slightly vary. For instance, the concentrations of all elements in the Co–Cr–Fe–Ni combinatorial sample processed by MBS technique varied between ≈ 5 and ≈ 61 at% on the surface of the film deposited on a single-crystal silicon wafer with the diameter of about 100 mm.^[15,22] It is worth noting, however, that the film thickness was only about 1 μm and the microstructure has a nanocrystalline character with the grain size of $\approx 10\text{--}20$ nm, irrespectively of the composition which suggests a nonequilibrium state of the material (due to the large amount of grain boundaries

and other defects). Thus, the phase composition may also differ from the thermodynamically stable one. Combinatorial films on reasonably large substrates have also been produced in other MPEA systems such as Fe–Mn–Co–Cr–Al, Co–Cr–Fe–Mn–Ni, Al–Co–Cr–Fe–Ni, and Ag–Ir–Pd–Pt–Ru using codeposition methods.^[12,27–29]

AM techniques are also used to produce combinatorial MPEA samples. In this case, the powders of a pre-alloyed MPEA and another foreign element or alloy are mixed with the desired fractions, and the powder blend is in-situ alloyed and consolidated using a laser beam.^[26,30] Changing the ratio of the two constituent powders during the deposition of the specimen layer by layer, a broad range of MPEA compositions can be synthesized in a single metallurgical sample. For instance, using prealloyed CoCrFeMnNi HEA and Nb powders, combinatorial $\text{Nb}_x[\text{CoCrFeMnNi}]_{1-x}$ MPEA specimen was created by laser beam-directed energy deposition.^[26] The atomic fraction of Nb increased with 1 at% from layer to layer which corresponds to a distance of about 100 μm . The Nb content varied between 0% and 100%; however, the ratio of the concentrations of the constituents of the prealloyed HEA (e.g., Co, Cr, and Fe) did not change in the sample, that is, the full compositional library in the Co–Cr–Fe–Mn–Ni–Nb system cannot be studied in this 3D-printed sample. This is a deficiency of the AM-processed combinatorial MPEA specimens similar to the diffusional couples (see above). Moreover, the 3D-printed materials often contain defects such as lack-of-fusion, cracks, and pores which weaken the strength and may result in an incomplete dissolution of the foreign element in the prealloyed HEA.^[26,31,32] Indeed, particles of pure Nb can be found in the as-processed combinatorial $\text{Nb}_x[\text{CoCrFeMnNi}]_{1-x}$ MPEA sample due to the incomplete melting of Nb powder.^[26] In addition, the fast cooling in the laser-assisted processing can yield large residual stresses and many lattice defects (e.g., dislocations and grain boundaries) in 3D-printed materials which may influence the observed phase composition. It is noted that pre-existing MPEAs can be alloyed by AM not only in powder form but also as a bulk substrate. For instance, a compositional $\text{Al}_x\text{CoCrFeNi}$ ($x = 0.15\text{--}1.32$) MPEA library was produced by laser-assisted alloying of an equiatomic CoCrFeNi substrate with varying amounts of Al powder.^[33] These MPEAs with different compositions were processed in patches with the size of 2 mm on the surface of the substrate; therefore, these areas were large enough for XRD phase analysis. The Al content varied with the step size of ≈ 0.05 in x ($\text{Al}_x\text{CoCrFeNi}$) which corresponds to the concentration of about 0.8 at%. In AM-processed $\text{Al}_x\text{CoCrFeNi}_2$ MPEA, 1 at% change in the concentration of Al corresponds also to a relatively high distance of about 1 mm; therefore, its phase composition can be studied by laboratory XRD.^[30] Indeed, as an example, **Figure 1a** shows the phase composition of the AM-processed combinatorial $\text{Al}_x\text{CoCrFeNi}_2$ MPEA as a function of the Al content.^[30] In this material, the phase composition was successfully tailored by changing the Al concentration. Namely, with increasing the amount of Al, the fraction of the disordered and ordered ($L1_2$) face-centered cubic (fcc) structures decreased while the fraction of the disordered and ordered (B2) body-centered cubic (bcc) phases increased. Nevertheless, a weakness of AM techniques is that they are not suitable to

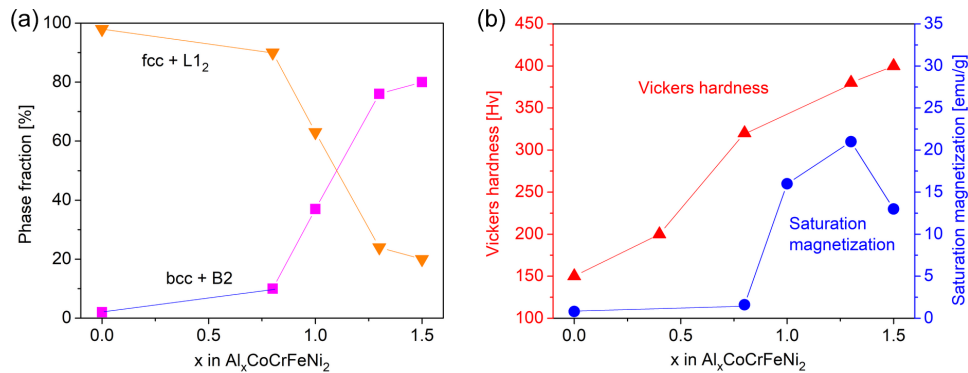


Figure 1. a) The phase fractions as a function of the Al content in an AM-processed combinatorial Al_xCoCrFeNi₂ MPEA sample. b) The variation of the Vickers hardness and the saturation magnetization versus the amount of Al. The data were taken from ref. [30].

Table 1. Comparison of some features of the three main processing techniques of combinatorial MPEAs.

Processing method	Length scale of concentration variation [$\mu\text{m at}\%^{-1}$]	Concentration range of elements [at%]	Thermal equilibrium
Diffusion couples	2–3	0–100, for a single component	yes
Film sputtering	2000–3000	5–60, for all components	no
AM	100–1000	0–100, for a single component	no

produce such combinatorial MPEA samples in which all constituents vary in a broad range since always prealloyed MPEAs are used in the material processing (similar to the diffusion couple technique). **Table 1** compares some features of the three main processing techniques of combinatorial MPEAs.

3. Characterization of Combinatorial MPEAs

XRD is an easy-to-perform and nondestructive way to characterize the crystalline phase composition in combinatorial MPEAs. The typical diameter of the illuminated area on the sample surface for laboratory XRD is about 1 mm, but at synchrotron 1–2 orders of magnitude smaller X-ray spot size can be achieved. Therefore, a structural mapping can be performed in the compositional library with the concentration resolution of about 1 at%. In addition, at synchrotron, the acquisition time of an XRD pattern is very short (less than 10 s); therefore, a complete mapping of a combinatorial MPEA sample can be performed within an hour even if a few hundreds of diffractograms have to be measured. The traditional evaluation of the patterns takes a much longer time than the measurement; however, fast artificial intelligence (AI)-based methods have been elaborated recently for a fast identification of the crystalline phases from the X-ray diffractograms.^[34–39] Using these techniques, the structural mapping of combinatorial MPEAs is easy and time saving.

AI has also brought a revolution in the characterization of the microstructure for combinatorial MPEAs. Namely, a machine learning-based X-ray line profile analysis (ML-XLPA) method

was developed for the fast mapping of the microstructural parameters (e.g., crystallite size and lattice defect density) from the XRD patterns measured by synchrotron radiation.^[39] During XLPA, the width and shape of XRD profiles are evaluated which can yield the crystallite size distribution, the density, and the edge/screw character of dislocations as well as the planar fault probability in MPEAs.^[40] These parameters are sensitive to the chemical composition of MPEAs as it has been revealed by former studies.^[10,11,41] Combining synchrotron radiation experiment with ML-XLPA, a full microstructure mapping of combinatorial samples can be performed within hours. For instance, in a former study, a combinatorial Co–Cr–Fe–Ni MPEA film processed by MBS was investigated by synchrotron XRD with the step size of about 2–4 mm, which corresponded to a compositional resolution of about 1 at%.^[39] **Figure 2** shows the phase map obtained from the evaluation of the XRD patterns measured on the disk with the diameter of 10 cm. The largest area was related to pure fcc phase; therefore, an ML-XLPA procedure was developed for the determination of maps of microstructural parameters which included the analysis of hundreds of diffractograms which would have been impossible with classical evaluation methods in a reasonable time. Beside the newly developed AI-based XRD and XLPA techniques, classical methods for microstructure investigation were also applied on combinatorial MPEA samples. For instance, scanning electron microscopy (SEM), transmission electron microscopy (TEM), and electron backscatter diffraction (EBSD) were used for microstructural study of different MPEA combinatorial compositions.^[30,33,42] The latter techniques yield orders of magnitude higher resolution in the microstructure investigation than XRD, which is advantageous for the combinatorial specimens prepared by diffusion couples where usually 1 at% change in concentration corresponds to a distance of $\approx 2\text{--}3\ \mu\text{m}$ only (see above). It should be noted, however, that the sample preparation for SEM, EBSD, and TEM methods is more complicated and time-consuming than for XRD, especially when the microstructure should be studied in hundreds or thousands of points with different compositions.

The phase maps obtained experimentally on combinatorial MPEA samples can be compared with those determined theoretically. The theoretical phase composition of MPEAs can be obtained by thermodynamical calculations using CALPHAD,

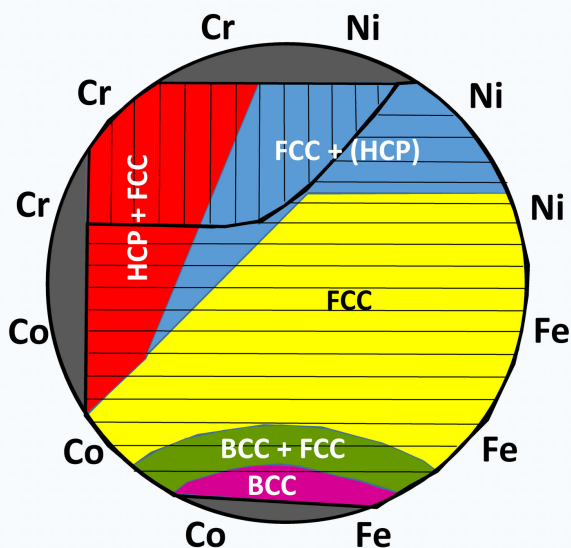


Figure 2. Phase map of a combinatorial Co–Cr–Fe–Ni MPEA film sample sputtered by MBS technique on a single-crystal Si substrate. More details on the sample processing and phase determination procedure can be found in ref. [15]. The acronyms of the constituents at the perimeter of the disk indicate the approximate positions of the 12 pure elemental sources. The gray color represents those parts of the substrate which were not covered by MPEA film. The colored areas indicate regions with various phase compositions. The areas with VEC values lower and higher than 8 are marked with vertical and horizontal stripes, respectively.

AI-based predictions or using simple empirical rules such as the relationship between the phase content and the valence electron concentration (VEC).^[21,43–50] Indeed, former studies suggested that VEC has a deterministic effect on the types of phases formed in different MPEA systems.^[51–53] Namely, when VEC is higher than about 8, an fcc phase forms while when VEC is lower than about 7 the stable phase has a bcc structure. Between these two VEC values, fcc and bcc phases coexist. In this rule, VEC is calculated as the average of the VEC values of the constituent elements weighted with their atomic fractions.^[53] In the experimental Co–Cr–Fe–Ni MPEA phase map shown in Figure 2, the areas marked with vertical and horizontal stripes correspond to VEC values between 7.5 and 8, and higher than 8, respectively. Thus, the VEC analysis predicts a single-phase fcc structure in the latter region while the coexistence of fcc and bcc phases is suggested in the former part of the combinatorial disk. The VEC-based prediction is false for the vertically striped region ($7.5 < \text{VEC} < 8$) since the fcc phase coexists with a hexagonal-close-packed (hcp) structure instead of a bcc phase. For $8 < \text{VEC}$, most of the horizontally striped area is occupied by the predicted fcc structure. On the other hand, hcp and bcc phases also formed in this region, although pure bcc structure is suggested to develop only if VEC is lower than about 7. This contradiction is not solved even if the revisited VEC rule is used which suggests that bcc structure is stable in the VEC range between 5 and 6.87.^[54] Most probably, the phases formed during sputtering are not in thermodynamic equilibrium; therefore, they do not follow the traditional structural predictions. In the

future, it is worth studying the influence of the processing way on the phase composition and the microstructure of MPEAs beside the effect of the chemistry, and the phase prediction methods must be improved accordingly.

In addition to the investigation of the phase composition and the microstructure, the mechanical and physical properties versus the element concentrations in combinatorial MPEAs can also be studied. The easiest way of the mechanical characterization of combinatorial samples is nanoindentation which can yield the nanohardness and the elastic modulus as a function of the chemical composition.^[15,26,55] The advantage of this technique is the very local characterization of the mechanical behavior, which can result in a fine resolution of the hardness and elastic modulus in MPEA compositional libraries. However, there are two shortcomings: 1) for low loads (small indents), an elevated hardness is obtained (called as indentation size effect) and 2) indentation yields an additional 8% strain. Both effects inhibit the determination of the bulk yield strength from the nanohardness value. Thus, as a future direction of mechanical testing of combinatorial samples, micropillar compression test is suggested to perform, although this method requires fabrication of pillars using focused ion beam technique which is expensive and takes time when a broad range of MPEA compositions is mapped. Besides the strength, the ductility is also a very important mechanical parameter; however, this can be obtained from tensile testing which is difficult to perform on a combinatorial sample. In the future, if AM is improved for manufacturing large combinatorial MPEA specimens with a reasonably low concentration gradient (about 1 at\% mm^{-1}), miniature tensile specimens with different compositions could be fabricated and tested by the recently developed high-throughput tensile testing rig which is capable of testing 60 specimens per hour.^[56]

Although, the effect of chemical composition of MPEAs on their physical (e.g., magnetic) properties has been extensively studied,^[57,58] these investigations were usually carried out on individual samples and not on combinatorial specimens. Only a few studies are available in the literature which performed their analysis on compositionally graded MPEA samples. For instance, combinatorial $\text{Al}_x\text{CoCrFeNi}_2$ ($0 \leq x \leq 1.5$) and $\text{AlCo}_x\text{Cr}_{1-x}\text{FeNi}$ ($0 \leq x \leq 1$) MPEAs were manufactured by AM, and then the saturation magnetization and the coercivity were studied as a function of the chemical composition.^[30,58] As an example, Figure 1b shows the variation of the hardness and the saturation magnetization as a function of the Al content in $\text{Al}_x\text{CoCrFeNi}_2$ ($0 \leq x \leq 1.5$) MPEA.^[30] The hardness increases with increasing the amount of Al due to the enhanced fraction of the hard bcc phase. Since the fcc and ordered L_{12} phases are nonmagnetic or weakly ferromagnetic, the increase of the fraction of the ferromagnetic bcc and B2 structures for a higher Al content yielded a greater saturation magnetization even if Al is paramagnetic. On the other hand, the saturation magnetization was reduced when the Al content increased from $x = 1.3$ to 1.5, which can be explained by the decrease of the fraction of the ordered B2 phase.^[30] It is noted that additional efforts should be made for a more extensive application of the physical characterization methods on combinatorial MPEA samples. For this purpose, the improvement of the existing characterization methods and the elaboration of novel techniques may be required since very

local measurements must be performed in order to achieve a fine compositional resolution of the investigations.

It is worth noting that in addition to the metallic MPEAs, high-entropy ceramics such as carbides and oxides have also been developed recently.^[59–64] The main goal of this invention is to obtain an extremely high strength even at very high temperatures (1000–2000 K). Indeed, it was found that high-entropy (Ti–Zr–Hf–V–Nb–Ta)C ceramic had a significantly higher hardness than the monocarbides of the constituent metallic elements.^[65] The elevated hardness was caused by the disordered multicomponent structure of high-entropy carbides which increases the critical resolved shear stress necessary for the slip of dislocations, and this effect was enhanced with increasing the number of metallic elements in the carbide.^[64] High-entropy carbides were processed in both bulk and coating forms.^[60,65] The bulk high-entropy carbides were formed by milling and subsequent spark plasma sintering of monocarbides. The remaining porosity after consolidation was less than 1 vol%. The chemical composition of high-entropy carbides has a significant effect on the active slip systems and thus on the deformability of these materials. Therefore, high-entropy carbides are candidates for ductile and high-strength ceramics.^[64] It should be noted, however, that combinatorial samples for high-entropy ceramics are not available yet, although they would facilitate the exploration of the ideal composition for the desired combination of the mechanical properties.

4. Complementary Theoretical Approaches of Combinatorial Design of MPEAs

It is also worth noting that the experimentally studied compositional libraries are often narrowed by preliminary theoretical calculations using DFT, MD, ML, or CALPHAD methods.^[16–21,66–69] However, this study focuses on the experimental part of the combinatorial design of MPEAs; therefore, only a brief overview of this theoretical field is given here. The high-throughput computational techniques can help to identify the compositions promising from the point of view of application demands, thereby reducing the time and effort invested in the experimental investigations. Using theoretical calculations, the phase composition and the properties (e.g., hardness, strength, or elastic modulus) can be predicted as a function of the concentration of constituent elements.^[70–73] As an example, **Figure 3** shows the hardness predicted by ML versus the experimentally determined values for some MPEA compositions. The power of ML method in maximizing the hardness of HEAs was demonstrated in the seven-component Al–Co–Cr–Cu–Fe–Ni–V alloy system.^[16] ML was trained using previously determined experimental hardness values for different compositions. Then, the five most crucial factors, such as the mean melting point of the alloy constituents, their average VEC, and the mean difference between their atomic weights influencing the hardness were determined. ML predicted the highest hardness with the value of about 10 GPa for the composition $\text{Co}_{18}\text{Cr}_7\text{Fe}_{35}\text{Ni}_5\text{V}_{35}$ which was confirmed experimentally. The measured hardness for this HEA composition was about 11.5 GPa which was significantly higher than any value in the training dataset; thus, ML was able to find a composition with a better hardness than measured ever before in the Al–Co–Cr–Cu–Fe–Ni–V alloy system. It

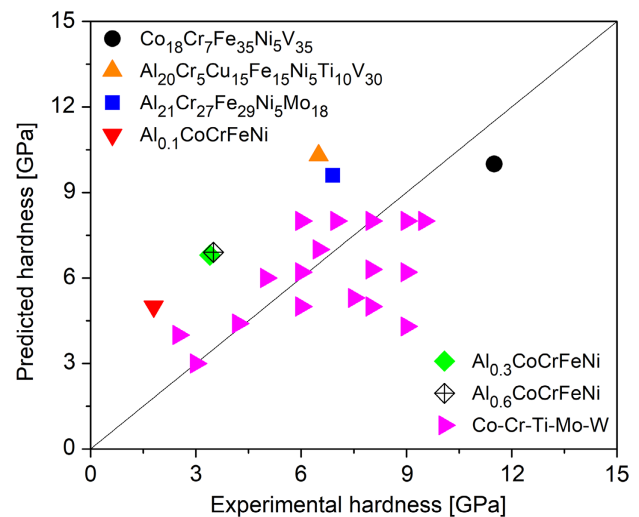


Figure 3. The hardness predicted by ML versus the experimentally determined values for some MPEA compositions. The data were taken from refs. [16,70].

seems that ML is capable for the prediction of the phase composition from the element concentrations as input parameters.^[44,74] The weakness of ML is that this method requires a large training dataset which is very rarely available in the literature. One big dataset of the phase composition and the mechanical properties is accessible in ref. [75].

Since the availability of large data sets required for training ML models is limited for novel HEAs, other theoretical methods, such as DFT, MD, and CALPHAD have a high significance in discovering new compositional libraries as well as narrowing the element concentration space necessary to study experimentally. Another advantage of the latter calculation techniques is that they have a strong physical background while ML is a statistical approach only. On the other hand, ML is more versatile in the prediction of different features and less time-consuming than other theoretical methods. First-principles calculations, such as DFT, can be successfully used to calculate the formation energy of different crystal structures for a given MPEA composition, thereby predicting the thermodynamically stable phase content as demonstrated for, for example, the Al–Co–Cr–Fe–Ni system.^[18] These ab-initio methods are also capable of determining the elastic constants, thermophysical, magnetic, and other properties of HEAs as a function of their chemical composition.^[76–80]

Theoretical calculations can be combined with ML in order to achieve better success in the prediction of the crystal structure versus the chemical composition. For instance, MD simulation was used to produce training sets for ML mapping of the yield strength in Fe–Co–Cr–Ni–Mn and Cu–Fe–Cr–Co–Ni alloy systems.^[20,81] However, MD is rather used for calculating the variation of the mechanical performance of HEAs as a function of the chemistry, for example, in the Co–Cr–Fe–Ni or Al–Co–Cr–Fe–Ni compositional libraries.^[19,20,82–84] It should be noted that the results of MD obtained on the mechanical behavior may deviate from the experimental observations since MD simulations correspond to a very high strain rate (10^8 1/s<) which is unusual in experimental tests.^[84]

The experimental phase mapping in an MPEA compositional space can be effectively facilitated by phase diagram calculations using CALPHAD method. However, for a trustworthy theoretical phase prediction, a reliable thermodynamic database is needed for the constituent elements of the investigated MPEA system which is often not available. First-principle calculations or former experimental data obtained from the binary subsystems of the studied compositional space can help bridge this gap. For many HEA systems, the goal of CALPHAD calculations is to identify the compositions giving a single-phase state since this microstructure may provide unique properties. For instance, in Al–Cr–Mn–Nb–Ti–V, Al–Cr–Mo–Nb–Ti–V, Al–Cr–Fe–Ti–V, and Al–Cr–Mn–Mo–Ti MPEA libraries, CALPHAD was successfully used to determine the chemical compositions related to single-phase bcc structures which may have a high oxidation resistance, thereby reducing the compositional space needed to study experimentally.^[21] Similarly, in the Co–Cr–Fe–Mn–Ni alloy system, the solid solution structures with good mechanical properties were identified by CALPHAD for a broad compositional space in which all constituents had concentrations at least 10%.^[85] This calculation was performed in a wide temperature range between 500 and 2500 K. As a result, a new promising composition (Co₁₀Cr₁₂Fe₄₃Mn₁₈Ni₁₇) was found which has similar room-temperature mechanical properties as the well-known equimolar Cantor alloy while the high-temperature strength and ductility are better (at least up to the temperature of 873 K). On the other hand, it has been shown that HEAs with small secondary phase particles have a better combination of strength and ductility compared to the single-phase solid solutions.^[5,86–88] Therefore, CALPHAD calculations were also used to find the compositions related to multiphase structures with hardening precipitates (e.g., in the Al–Co–Cr–Fe–Ni system).^[89] CALPHAD was combined with ML in order to improve its power in the prediction of the phase content in HEA compositional libraries.^[90]

It is worth emphasizing that CALPHAD predicts the crystal structure in thermal equilibrium which usually can only be achieved at an appropriately high temperature and a long time. Therefore, the phase composition obtained experimentally for a given chemical composition may differ from the one predicted by CALPHAD calculation since the structure in the combinatorial samples may not be in thermal equilibrium, depending on the applied processing technique. Therefore, the experimental and theoretical investigation methods should be used in a complementary way for exploring new MPEA compositions in combinatorial samples.

5. Summary and Future Research Directions

Combinatorial samples are of great importance in the selection of the optimal MPEA compositions since the processing and characterization of compositional libraries are much easier and faster when combinatorial specimens are used. Combinatorial MPEAs can be produced by different techniques such as diffusion couples, AM, and film sputtering. Very different composition gradients can be achieved by these methods. Namely, 1 at% change in the constituent concentration corresponds to the distance of 2–3, 100–1000 μm, and 2–3 mm for diffusion couples,

AM-processed bulk samples, and sputtered films, respectively. This difference has an impact on the applicability of microstructure characterization techniques. For instance, due to the relatively large beam size of laboratory XRD can be used for phase mapping with high-concentration resolution in the case of sputtered films but not for diffusion couples.

A nearly full compositional library has been obtained only in films produced by sputtering of pure constituents. In the other two techniques (diffusion couples and AM), mostly a pre-existing MPEA is alloyed with an additional element, that is, only a restricted part of the compositional library can be mapped using these samples. Another disadvantage of AM method is that sometimes the alloying is not completed; thus, particles of the added element may remain in the final specimen. On the other hand, it is beneficial that the techniques of diffusion couples and AM can produce bulk combinatorial samples while the thickness of the sputtered films is only a few micrometers. In addition, MPEA thin films usually have a nanocrystalline microstructure with high density of lattice defects, that is, they are far from equilibrium. It was revealed that the phase composition in a sputtered MPEA layer may differ significantly from the predicted one since the deposited material is not in an equilibrium state. As a future research direction, it would be important to study the effect of sputtering conditions on the phase composition and microstructure of MPEA films. Moreover, besides sputtering, other techniques must be made applicable for producing MPEA layers. For instance, the processing and characterization of combinatorial MPEA compositions processed by electroplating is missing from the literature.

The processing procedures of combinatorial MPEAs can be completed with an additional step: short time annealing at moderate temperatures. Indeed, it has been shown recently that such heat treatments can cause an improvement of the mechanical strength of bulk MPEAs. The phenomenon is called as anneal hardening and caused by the relaxation of lattice defect structure and/or local chemical ordering in MPEAs. Such an effect may also work in combinatorial samples, although the time and temperature of heat treatment must be selected carefully in order to avoid significant reduction of the concentration gradient.

Beside metallic MPEAs, high-entropy oxide and carbide ceramics are also promising candidates in different applications. On the other hand, combinatorial samples have not been processed yet for high-entropy ceramics; therefore, this is also a challenging technological task in the future. A possible solution for producing combinatorial high-entropy carbide ceramics may be the addition of a carbon source to the metallic sputtering targets in MBS technique. However, in this case the contamination of the PVD chamber with carbon is a critical issue since this element is hard to remove from the parts of the MBS device.

In addition to the novel processing techniques, new characterization methods of combinatorial MPEAs must be elaborated for an easier and faster description of these materials. Recently, an ML-based XRD analysis has been developed for a quick and reliable description of the microstructure by evaluating a very large number of synchrotron XRD patterns in a short time. The ML-XLPA method has been elaborated only for fcc materials; therefore, it is suggested to extend its applicability to other structures such as bcc and hcp, and also to multiphase MPEAs. ML-based methods can also be used for the identification of the phase

content from the X-ray diffractograms in a compositional library. In addition, AI is applied for the theoretical prediction of the phases from the chemical composition of MPEAs. Thus, it is expected that the role of ML will further increase in the theoretical and experimental studies of MPEA libraries. A complementary application of experimental techniques and theoretical calculations is suggested when new MPEA compositions with desired properties are searched.

Acknowledgements

The author thanks his colleagues who were cooperation partners in his research in the field of combinatorial MPEAs.

Conflict of Interest

The author declares no conflict of interest.

Author Contributions

J.G.: Writing – original draft, Conceptualization.

Keywords

combinatorial samples, hardnesses, high-entropy alloys, microstructures, multiprincipal element alloys

Received: October 12, 2023

Revised: December 3, 2023

Published online:

- [1] B. Cantor, I. T. H. Chang, P. Knight, A. J. B. Vincent, *Mater. Sci. Eng., A* **2004**, 375–377, 213.
- [2] J. W. Yeh, S. K. Chen, S. J. Lin, J. Y. Gan, T. S. Chin, T. T. Shun, C. H. Tsau, S. Y. Chang, *Adv. Eng. Mater.* **2004**, 6, 299.
- [3] J. W. Yeh, *JOM* **2013**, 65, 1759.
- [4] Y. Zhang, T. T. Zuo, Z. Tang, M. C. Gao, K. A. Dahmen, P. K. Liaw, Z. P. Lu, *Prog. Mater. Sci.* **2014**, 61, 1.
- [5] J. Gubicza, P. T. Hung, *Mater. Trans.* **2023**, 64, 1284.
- [6] O. N. Senkov, G. B. Wilks, J. M. Scott, D. B. Miracle, *Intermetallics* **2011**, 19, 698.
- [7] P. Edalati, R. Floriano, A. Mohammadi, Y. Li, G. Zepon, H. W. Li, K. Edalati, *Scr. Mater.* **2020**, 178, 387.
- [8] A. Mohammadi, Y. Ikeda, P. Edalati, M. Mito, B. Grabowski, H. W. Li, K. Edalati, *Acta Mater.* **2022**, 236, 118.
- [9] P. Edalati, M. Fujii, K. Edalati, *Rare Met.* **2023**, 42, 3246.
- [10] A. K. Chandan, K. Kishore, P. T. Hung, M. Ghosh, S. G. Chowdhury, M. Kawasaki, J. Gubicza, *Int. J. Plast.* **2022**, 150, 103193.
- [11] K. Kishore, A. K. Chandan, P. T. Hung, S. Kumar, M. Kawasaki, J. Gubicza, *Int. J. Plast.* **2023**, 169, 103720.
- [12] V. Dolique, A. L. Thomann, P. Brault, Y. Tessier, P. Gillon, *Surf. Coat. Technol.* **2010**, 204, 1989.
- [13] P. Nagy, N. Rohbeck, Z. Hegedűs, J. Michler, L. Pethő, J. L. Lábár, J. Gubicza, *Materials* **2021**, 14, 3357.
- [14] S. Mooraj, W. Chen, *J. Mater. Inf.* **2023**, 3, 4.
- [15] P. Nagy, N. Rohbeck, R. Widmer, Z. Hegedűs, J. Michler, L. Pethő, J. L. Lábár, J. Gubicza, *Materials* **2022**, 15, 2319.
- [16] C. Yang, C. Ren, Y. Jia, G. Wang, M. Li, W. Lu, *Acta Mater.* **2022**, 222, 117431.
- [17] Y. V. Krishna, U. K. Jaiswal, R. M. Rahul, *Scr. Mater.* **2021**, 197, 113804.
- [18] V. Sorkin, Z. G. Yu, S. Chen, T. L. Tan, Z. H. Aitken, Y. W. Zhang, *Sci. Rep.* **2022**, 12, 11894.
- [19] J. Li, B. Xie, Q. Fang, B. Liu, Y. Liu, P. K. Liaw, *J. Mater. Sci. Technol.* **2021**, 68, 70.
- [20] L. Zhang, K. Qian, J. Huang, M. Liu, Y. Shibuta, *J. Mater. Res. Technol.* **2021**, 13, 2043.
- [21] T. P. C. Klaver, D. Simonovic, M. H. F. Sluiter, *Entropy* **2018**, 20, 911.
- [22] P. Nagy, N. Rohbeck, G. Rouselly, P. Sortais, J. Gubicza, J. Michler, L. Pethő, *Surf. Coat. Technol.* **2020**, 386, 125465.
- [23] T. Keil, E. Bruder, K. Durst, *Mater. Des.* **2019**, 176, 107816.
- [24] T. Keil, D. Utt, E. Bruder, A. Stukowski, K. Albe, K. Durst, *J. Mater. Res.* **2021**, 36, 2558.
- [25] Y. Shi, B. Yang, P. D. Rack, S. Guo, P. K. Liaw, Y. Zhao, *Mater. Des.* **2020**, 195, 109018.
- [26] J. W. Pegues, M. A. Melia, R. Puckett, S. R. Whetten, N. Argibay, A. B. Kustas, *Addit. Manuf.* **2021**, 37, 101598.
- [27] A. Marshal, K. G. Pradeep, D. Music, L. Wang, O. Petravic, J. M. Schneider, *Sci. Rep.* **2019**, 9, 7864.
- [28] A. Kauffmann, M. Stüber, H. Leiste, S. Ulrich, S. Schlabach, D. V. Szabó, S. Seils, B. Gorr, H. Chen, H. J. Seifert, M. Heilmayer, *Surf. Coat. Technol.* **2017**, 325, 174.
- [29] L. Gao, W. Liao, H. Zhang, J. U. Surjadi, D. Sun, Y. Lu, *Coatings* **2017**, 7, 156.
- [30] T. Borkar, B. Gwalani, D. Choudhuri, C. Mikler, C. Yannetta, X. Chen, R. V. Ramanujan, M. Styles, M. Gibson, R. Banerjee, *Acta Mater.* **2016**, 116, 63.
- [31] A. Hattal, K. Mukhtarova, M. Djemai, T. Chauveau, A. Hocini, J. J. Fouchet, B. Bacroix, J. Gubicza, G. Dirras, *Mater. Des.* **2022**, 214, 110392.
- [32] B. Guennec, A. Hattal, A. Hocini, K. Mukhtarova, T. Kinoshita, N. Horikawa, J. Gubicza, M. Djemai, G. Dirras, *Int. J. Fatigue* **2022**, 164, 107129.
- [33] M. Li, J. Gazquez, A. Borisevich, R. Mishra, K. M. Flores, *Intermetallics* **2018**, 95, 110.
- [34] F. Oviedo, Z. Ren, S. Sun, C. Settens, Z. Liu, H. N. T. Putri, S. Ramasamy, B. L. DeCost, S. I. P. Tian, G. Romano, A. G. Kusne, T. Buonassisi, *Comput. Mater.* **2019**, 5, 60.
- [35] Y. Liu, N. Marcella, J. Timoshenko, A. Halder, B. Yang, L. Kolipaka, M. J. Pellin, S. Seifert, S. Vajda, P. Liu, A. I. Frenkel, *J. Chem. Phys.* **2019**, 151, 164201.
- [36] K. Utimula, R. Hunkao, M. Yano, H. Kimoto, K. Hongo, S. Kawaguchi, S. Suwanna, R. Maezono, *Adv. Theory Simul.* **2020**, 3, 2000039.
- [37] Y. Suzuki, H. Hino, T. Hawaii, K. Saito, M. Kotsugi, K. Ono, *Sci. Rep.* **2020**, 10, 21790.
- [38] J. W. Lee, W. B. Park, J. H. Lee, S. P. Singh, K. S. Sohn, *Nat. Commun.* **2020**, 11, 86.
- [39] P. Nagy, B. Kaszás, I. Csabai, Z. Hegedűs, J. Michler, L. Pethő, J. Gubicza, *Nanomaterials* **2022**, 12, 4407.
- [40] J. Gubicza, *Eur. Phys. J.: Spec. Top.* **2022**, 231, 4153.
- [41] J. Gubicza, P. T. Hung, M. Kawasaki, J. K. Han, Y. Zhao, Y. Xue, J. L. Lábár, *Mater. Charact.* **2019**, 154, 304.
- [42] D. B. Miracle, M. Li, Z. Zhang, R. Mishra, K. M. Flores, *Annu. Rev. Mater. Res.* **2021**, 51, 131.
- [43] O. N. Senkov, J. D. Miller, D. B. Miracle, C. Woodward, *Nat. Commun.* **2015**, 6, 6529.
- [44] A. Nassar, A. Mullis, *Comput. Mater. Sci.* **2021**, 199, 110755.
- [45] S. Risal, W. Zhu, P. Guillen, L. Sun, *Comput. Mater. Sci.* **2021**, 192, 110389.
- [46] G. Y. Ke, S. K. Chen, T. Hsu, J. W. Yeh, *Ann. Chim.* **2006**, 31, 669.
- [47] S. Guo, C. T. Liu, *Prog. Nat. Sci.: Mater. Int.* **2011**, 21, 433.
- [48] S. Guo, C. Ng, J. Lu, C. Liu, *J. Appl. Phys.* **2011**, 109, 103505.

- [49] N. N. Guo, L. Wang, L. S. Luo, X. Z. Li, Y. Q. Su, J. J. Guo, H. Z. Fu, *Mater. Des.* **2015**, *81*, 87.
- [50] C. C. Juan, M. H. Tsai, C. W. Tsai, C. M. Lin, W. R. Wang, C. C. Yang, S. K. Chen, S. J. Lin, J. W. Yeh, *Intermetallics* **2015**, *62*, 76.
- [51] S. S. Mohd Pauzi, M. K. Harun, M. Talari, *Mater. Sci. Forum* **2016**, *846*, 13.
- [52] Q. Wei, Q. Shen, J. Zhang, B. Chen, G. Luo, L. Zhang, *Int. J. Refract. Met. Hard Mater.* **2018**, *77*, 8.
- [53] S. Yang, J. Lu, F. Xing, L. Zhang, Y. Zhong, *Acta Mater.* **2020**, *192*, 11.
- [54] S. Yang, G. Liu, Y. Zhong, *J. Alloys Compd.* **2022**, *916*, 165477.
- [55] L. Jiang, Z. Cao, J. Jie, J. J. Zhang, Y. P. Lu, T. M. Wang, T. J. Li, *J. Alloys Compd.* **2015**, *649*, 585.
- [56] K. Huang, C. Kain, N. Diaz-vallejo, Y. Sohn, L. Zhou, *J. Manuf. Process.* **2021**, *66*, 494.
- [57] Y. Tang, S. Sun, M. Lv, J. Zhu, Y. Tan, X. Tan, Y. Yang, H. Xu, *Intermetallics* **2021**, *135*, 107216.
- [58] T. Borkar, V. Chaudhary, B. Gwalani, D. Choudhuri, C. V. Mikler, V. Soni, T. Alam, R. V. Ramanujan, R. Banerjee, *Adv. Eng. Mater.* **2017**, *19*, 1700048.
- [59] Y. Zhang, *High-Entropy Materials: Advances and Applications*, CRC Press, Boca Raton, FL **2023**.
- [60] E. Castle, T. Csanádi, S. Grasso, J. Dusza, M. Reece, *Sci. Rep.* **2018**, *8*, 8609.
- [61] T. Csanádi, E. Castle, M. J. Reece, J. Dusza, *Sci. Rep.* **2019**, *9*, 10200.
- [62] Y. Wang, T. Csanádi, H. Zhang, J. Dusza, M. J. Reece, R. Z. Zhang, *Adv. Theory Simul.* **2020**, *3*, 2000111.
- [63] T. Csanádi, V. Girman, L. Maj, J. Morgiel, M. J. Reece, J. Dusza, *Int. J. Refract. Met. Hard Mater.* **2021**, *100*, 105646.
- [64] Y. Wang, T. Csanádi, H. Zhang, J. Dusza, M. J. Reece, *Acta Mater.* **2022**, *231*, 117887.
- [65] V. F. Gorban, A. A. Andreyev, G. N. Kartmazov, A. M. Chikryzhov, M. V. Karpets, A. V. Dolomanov, A. A. Ostroverkh, E. V. Kantsyr, *J. Superhard Mater.* **2017**, *39*, 166.
- [66] P. Sarker, T. Harrington, C. Toher, C. Oses, M. Samiee, J. P. Maria, D. W. Brenner, K. S. Vecchio, S. Curtarolo, *Nat. Commun.* **2018**, *9*, 4980.
- [67] K. Kaufmann, D. Maryanovsky, W. M. Mellor, C. Zhu, A. S. Rosengarten, T. J. Harrington, C. Oses, C. Toher, S. Curtarolo, K. S. Vecchio, *Comput. Mater.* **2020**, *6*, 42.
- [68] L. Chen, Z. Chen, X. Yao, B. Su, W. Chen, X. Pang, K. S. Kim, C. Veer Singh, Y. Zou, *J. Mater. Inf.* **2022**, *2*, 19.
- [69] H. Meng, R. Yu, Z. Tang, Z. Wen, Y. Chu, *Cell Rep. Phys. Sci.* **2023**, *4*, 101512.
- [70] G. Kim, H. Diao, C. Lee, A. T. Samaei, T. Phan, M. de Jong, K. An, D. Ma, P. K. Liaw, W. Chen, *Acta Mater.* **2019**, *181*, 124.
- [71] W. Huang, P. Martin, H. L. Zhuang, *Acta Mater.* **2019**, *169*, 225.
- [72] D. Dai, T. Xu, X. Wei, G. Ding, Y. Xu, J. Zhang, H. Zhang, *Comput. Mater. Sci.* **2020**, *175*, 109618.
- [73] A. Roy, T. Babuska, B. Krick, G. Balasubramanian, *Scr. Mater.* **2020**, *185*, 152.
- [74] Q. Wu, Z. Wang, X. Hu, T. Zheng, Z. Yang, F. He, J. Li, J. Wang, *Acta Mater.* **2020**, *182*, 278.
- [75] K. Christopher, H. Borg, C. Frey, J. Moh, T. M. Pollock, S. Gorsse, D. B. Miracle, O. N. Senkov, B. Meredig, J. E. Saal, *Sci. Data* **2020**, *7*, 430.
- [76] Y. Lederer, C. Toher, K. S. Vecchio, S. Curtarolo, *Acta Mater.* **2018**, *159*, 364.
- [77] L. Chen, X. Hao, Y. Wang, X. Zhang, H. Liu, *Mater. Res. Express* **2020**, *7*, 106516.
- [78] Z. Huang, Z. Li, D. Wang, Y. Shi, M. Yan, Y. Fu, *J. Phys. Chem. Solids* **2021**, *151*, 109.
- [79] S. Wang, J. Xiong, D. Li, Q. Zeng, M. Xiong, X. Chai, *Mater. Lett.* **2021**, *282*, 128754.
- [80] G. Ouyang, P. Singh, R. Su, D. D. Johnson, M. J. Kramer, J. H. Perepezko, O. N. Senkov, D. Miracle, J. Cui, *npj Comput. Mater.* **2023**, *9*, 141.
- [81] L. Zhang, K. Qian, B. W. Schuller, Y. Shibuta, *Metals* **2021**, *11*, 922.
- [82] J. Li, Q. Fang, B. Liu, Y. Liu, Y. Liu, *RSC Adv.* **2016**, *6*, 76409.
- [83] A. Jarlöv, W. Ji, Z. Zhu, Y. Tian, R. Babicheva, R. An, H. L. Seet, M. L. S. Nai, K. Zhou, *J. Alloys Compd.* **2022**, *905*, 164137.
- [84] J. Jiang, W. Sun, N. Luo, *Mater. Today Commun.* **2022**, *31*, 103861.
- [85] P. L. Conway, T. Klaver, J. Steggo, E. Ghassemali, *Mater. Sci. Eng., A* **2022**, *830*, 142297.
- [86] P. Edalati, A. Mohammadi, M. Ketabchi, K. Edalati, *J. Alloys Compd.* **2021**, *884*, 161101.
- [87] S. Zhao, Z. Li, C. Zhu, W. Yang, Z. Zhang, D. E. Armstrong, P. S. Grant, R. O. Ritchie, M. A. Meyers, *Sci. Adv.* **2021**, *7*, eabb3108.
- [88] P. Edalati, A. Mohammadi, Y. Tang, R. Floriano, M. Fujii, K. Edalati, *Mater. Lett.* **2021**, *302*, 130368.
- [89] A. Abu-odeh, E. Galvan, T. Kirk, H. Mao, Q. Chen, P. Mason, R. Malak, R. Arróyave, *Acta Mater.* **2018**, *152*, 41.
- [90] Y. Zeng, M. Man, K. Bai, Y. Zhang, *Mater. Des.* **2021**, *202*, 109532.



Jenő Gubicza is a professor at Department of Materials Physics, Eötvös Loránd University, Budapest, Hungary. He served as the head of his department and the Doctoral School of Physics. His special field is the study of the correlation between the microstructure and mechanical properties of advanced materials. He wrote three books about the defect structure and properties of nanomaterials as well as about X-ray line profile analysis which is an effective method for the study of the defect structure of materials.